Geomechanics Effects and Optimizations on Compositional Simulations of Gas Mobility Control Techniques for CO2 EOR

Xueying Lu

Joint work with

Mary F. Wheeler[1] and Mohammad Lotfollahi[2]

[1]The Center for Subsurface Modeling,

Oden Institute of Computational Engineering and Science, UT Austin

[2]ExxonMobil

Sept. 26, 2019

ODEN INSTITUTE
FOR COMPUTATIONAL ENGINEERING & SCIENCES

CSM
CENTER FOR SUBSURFACE MODELING

Outline

- ❑ **Introduction**
- ❑ Numerical Study of Gas Mobility Control Techniques in Cranfield
- ❑ Geomechanics Effects on Gas Mobility Control Techniques
- ❑ Optimization of Surfactant Alternating Gas (SAG) Process
- ❑ Conclusions

Motivation

- Foam has been proven to be effective for flood conformance control during EOR and CO_2 storage processes.
  - Reduces liquid/gas mobility ratio
  - Blocks gas migration along high permeability pathways

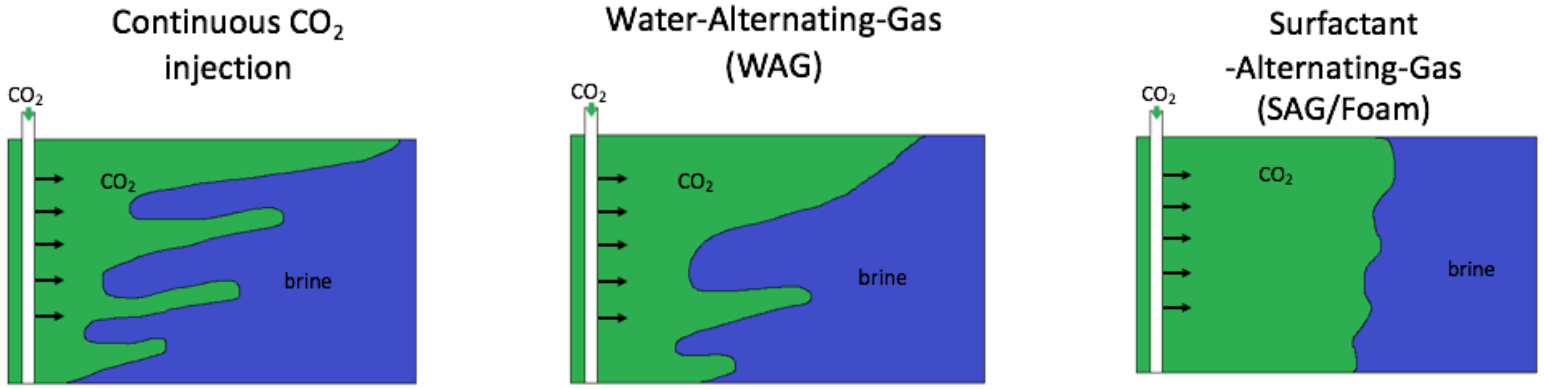

- Coupled compositional flow-geomechanics model can
  - Examine the geomechanics effects on flow
  - estimate the pressure margin for inducing fracturing to ensure secure operations.

Simulation Workhorse - IPARS

Flow
- **Compositional**
- Black Oil
- Single & Two Phase

Geomechanics
- **Poroelasticity**
- Poroplasticity

Reactive Transport
- TRCHEM
- ASP Flooding

Models

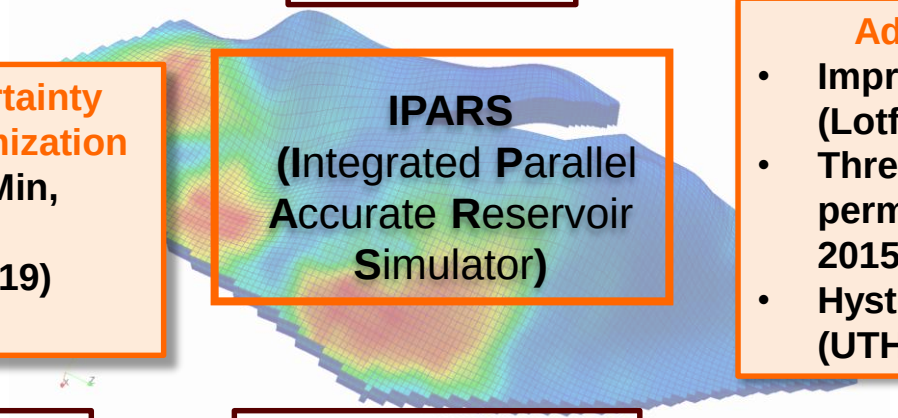

IPARS
(Integrated Parallel Accurate Reservoir Simulator)

History Match, Uncertainty Quantification & Optimization
- **Multi-objective GA (Min, 2017)**
- **CMA-ES (Lu et al, 2019)**
- EnKF

Advanced Petrophysics
- **Improved CMG STARS Foam (Lotfollahi 2017)**
- **Three phase relative permeability (UTKR3P, Beygi 2015)**
- **Hysteretic relative permeability (UTHYST, Beygi 2015)**

General Geometrics
- General Hexahedral
- Bricks
- Unstructured meshes
- Dynamic meshes

Solvers/Packages
- SAMG
- GMRES
- BCGS
- TRILINOS
- HYPRE

Interface
I/O
Visualization
- Paraview
- Tecplot

Compositional Flow Model

- 3-Phases: $\alpha \in \{o, w, g\}$, N_c-Components: $i \in \{w, 2, \ldots, N_c\}$.
- Flash calculation for hydrocarbon phase behavior (Peng-Robinson EOS).
- Hydrocarbons are fully compressible, water is slightly compressible.
- Mass Conservation of component i:

$$\frac{\partial}{\partial t}\left(\sum_{\alpha} \phi S_{\alpha} \rho_{\alpha} \xi_{i\alpha}\right) + \nabla \cdot \sum_{\alpha} \left(\rho_{\alpha} \xi_{i\alpha} u_{\alpha} - \phi S_{\alpha} D_{i\alpha} \cdot \nabla (\rho_{\alpha} \xi_{i\alpha})\right) = \sum_{\alpha} q_{i\alpha}, \quad \text{in } \Omega \times (0, T].$$

- Darcy's Law for phase α flux: $u_{\alpha} = -K \frac{k_{r\alpha}}{\mu_{\alpha}} (\nabla p_{\alpha} - \rho_{m,\alpha} g)$.

p_α	pressure	u_α	Darcy flux	$D_{i\alpha}$	diffusion-dispersion
S_α	saturation	$\xi_{i\alpha}$	mole fraction	μ_α	viscosity
ϕ	porosity	K	absolute permeability	$\rho_{m,\alpha}$	mass density
$q_{i\alpha}$	source/sink	$k_{r\alpha}$	relative permeability	g	gravity

- ❑ Introduction
- ❑ **Numerical Study of Gas Mobility Control Techniques in Cranfield**
- ❑ Geomechanics Effects on Gas Mobility Control Techniques
- ❑ Optimization of Surfactant Alternating Gas (SAG) Process
- ❑ Conclusions

Compositional Cranfield Model

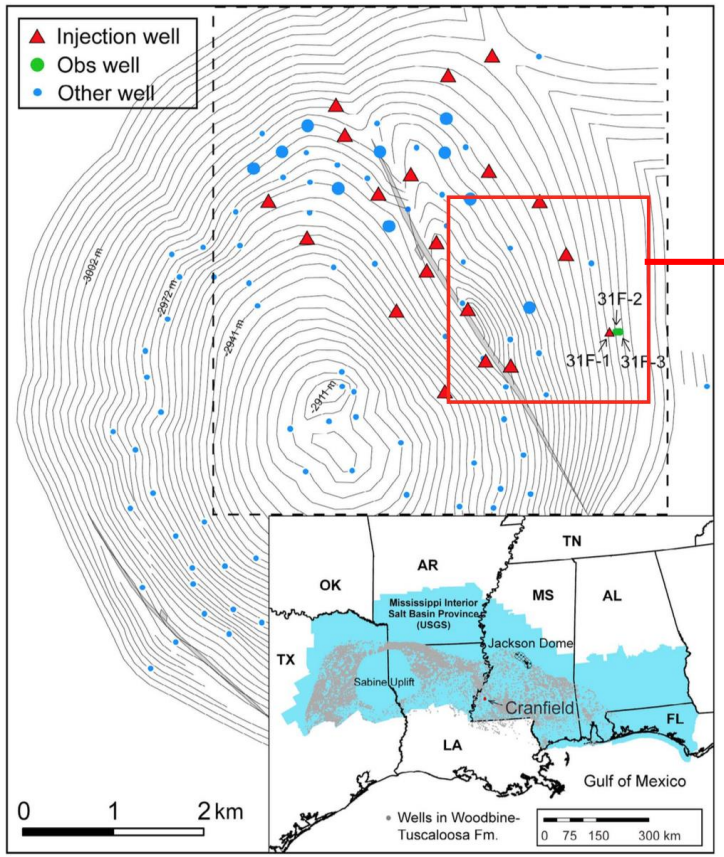

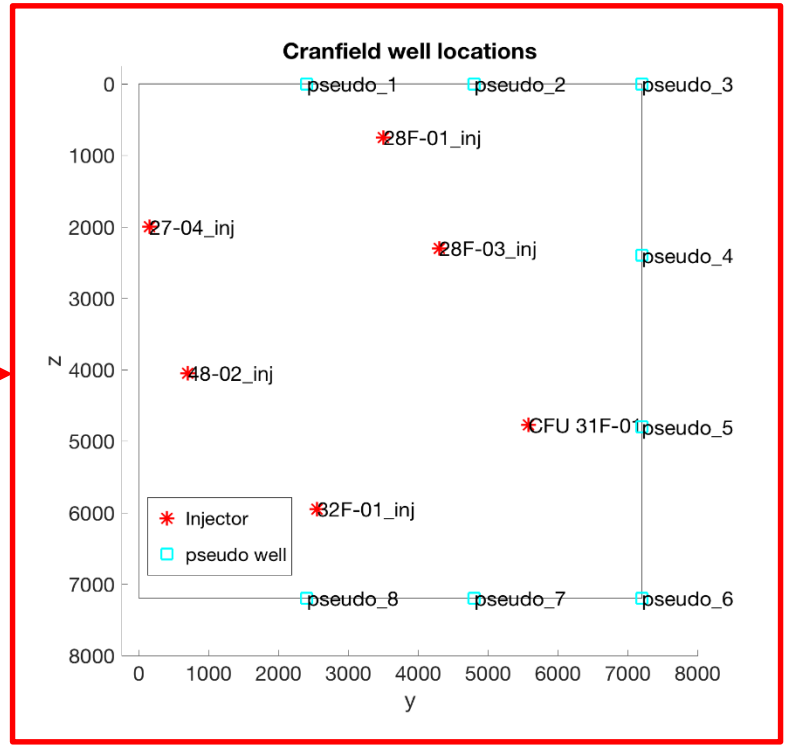

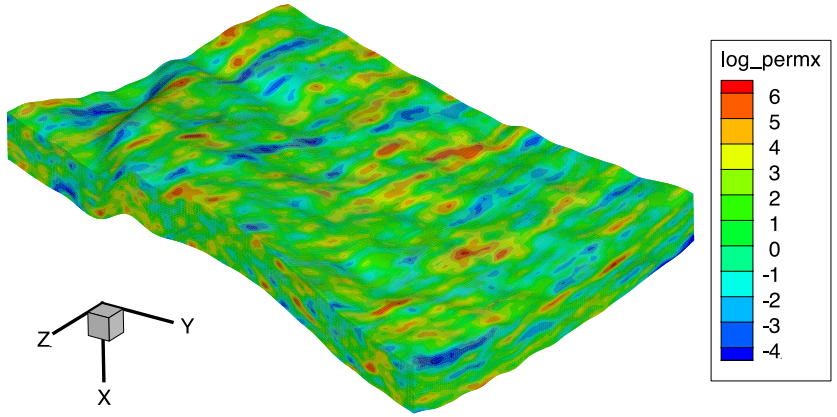

Numerical model of Cranfield field test	
Model type	Compositional model
Reservoir size	7200×7200×80 (ft)
Number of grid blocks	144×144×20
Initial water saturation	1.0
Initial reservoir pressure	4650 (psi)
Initial reservoir temperature	257 (°F)
Reservoir salinity	150,000 (ppm)

PVT data		
	CO_2	Brine
Critical temperature (°R)	547.56	1120.23
Critical pressure (psia)	1070.4	3540.9
Compressibility factor	0.255	0.2
Acentric factor	0.224	0.244
Molecular weight (g/g mol)	44.01	18.01
Volume-shift	-0.19	0.065
Binary interaction coefficients	0.09	0.09

Injection Schedules

- Continuous CO_2 injection

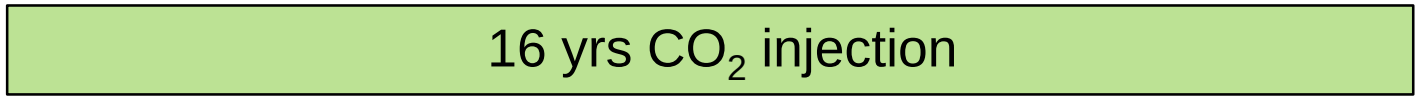

- WAG

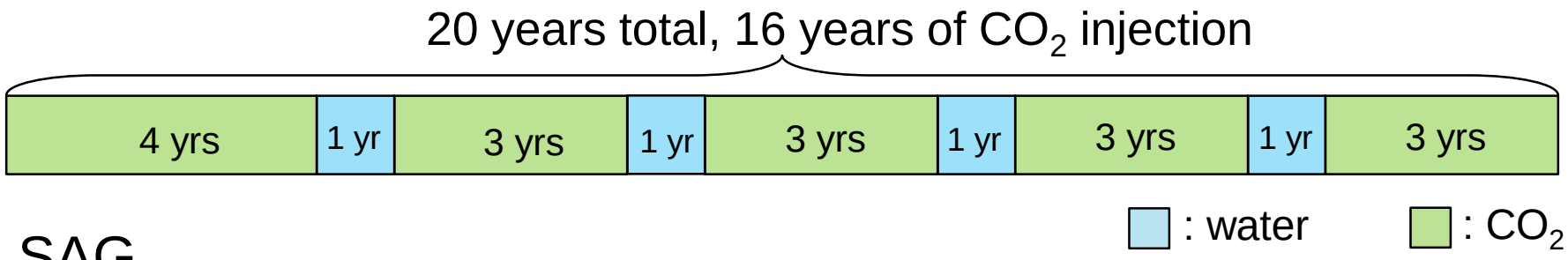

- SAG

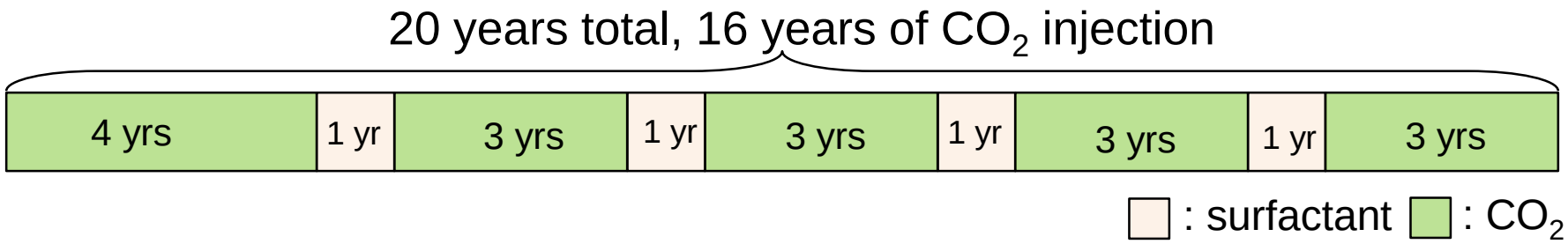

CO_2 Saturation Distribution

- Continuous CO_2 Injection
- WAG with hysteresis
- SAG

Top view

Bottom view

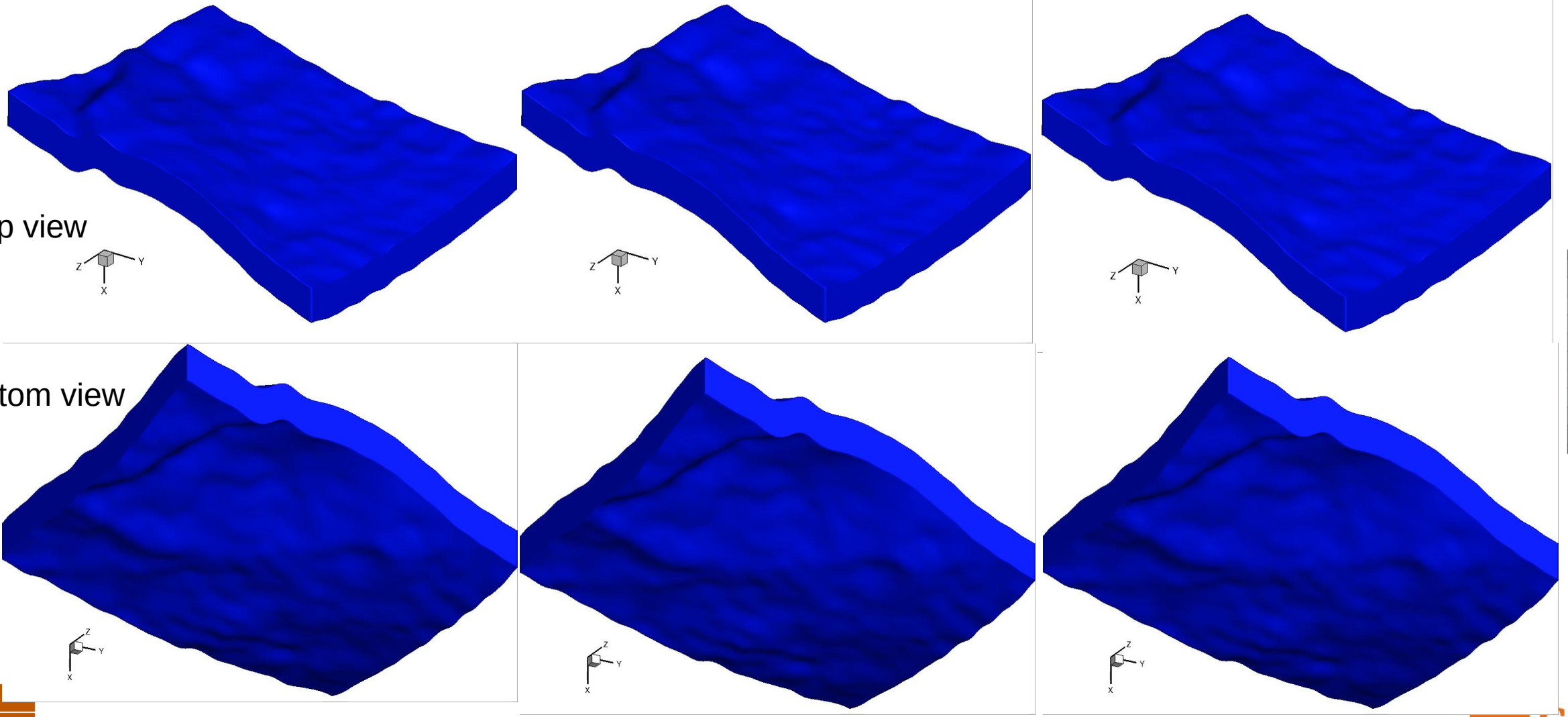

Field Statistics

Injection Scenario	CO_2 injection	WAG w/o hysteresis	WAG with hysteresis	SAG
Cum CO_2 injected (MMscf)	2.10E+05	2.10E+05	2.10E+05	2.10E+05
Cum CO_2 lost from boundaries (MMscf)	1.01E+05	1.12E+05	4.21E+04	1.71E+04
CO_2 lost from boundaries (%)	**48.2**	**53.1**	**20.0**	**8.1**

- In continuous CO_2 injection, 48.2% of the total injected CO_2 does NOT store inside the selected sector model and is produced through the boundaries.
- CO_2 lost from reservoir boundaries decreases from 48.2% to 20% and 8.1% using WAG and SAG processes, respectively.

- ❑ Introduction
- ❑ Numerical Study of Gas Mobility Control Techniques in Cranfield
- ❑ **Geomechanics Effects on Gas Mobility Control Techniques**
- ❑ Optimization of Surfactant Alternating Gas (SAG) Process
- ❑ Conclusions

Linear Poroelasticity

- Stress equilibrium equation

$$-\nabla \cdot \boldsymbol{\sigma}^{eff} = [\rho_s(1-\phi) + \phi(\rho_o S_o + \rho_w S_w + \rho_g S_g)]\boldsymbol{g},$$

$$\boldsymbol{\sigma}^{eff} = \boldsymbol{\sigma}^{tot} - \alpha p I.$$

- Constitutive equations

$$\boldsymbol{\sigma}^{tot} = \lambda(\nabla \cdot \boldsymbol{u})I + 2\mu\boldsymbol{\epsilon},$$

$$\boldsymbol{\epsilon} = \frac{1}{2}\left(\nabla \boldsymbol{u} + \nabla \boldsymbol{u}^T\right)$$

- Fixed stress iterative coupling to the compositional flow model

$$\phi = \phi_0 + \alpha(\varepsilon_v - \varepsilon_{v,0}) + \frac{1}{M}(p - p_0)$$

σ^{eff}	Effective stress tensor	p	Pore pressure
σ^{tot}	Total stress tensor	α	Boit's coefficient
ε	Strain tensor	E	Young's modulus
$\mathbf{u}$	Displacement vector	ν	Poisson's ratio

$$\lambda = \frac{\nu E}{(1+\nu)(1-2\nu)}$$

$$\mu = \frac{E}{2(1+\nu)}$$

Geomechanics Model

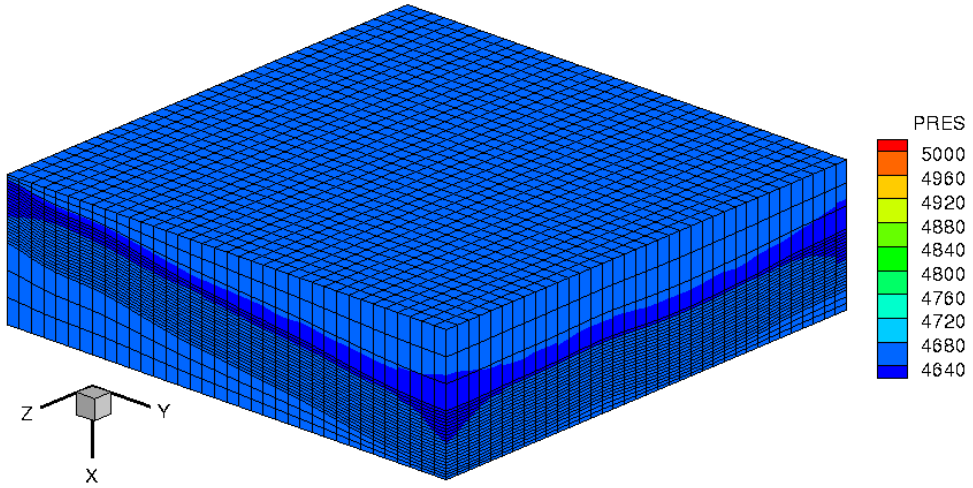

- Initial vertical stress 10054 psi, horizontal stress 7495 psi
- Normal traction of 10054 psi on the top face
- Zero normal displacements (roller boundary) on the rest five faces

Young's modulus and Poisson's ratio for the Cranfield model, courtesy to White et al., 2017

Facies	Layers	E (psi)	ν
Overburden	1 - 3	2.2E+06	0.25
C	4 - 6	1.45E+06	0.31
B	7 - 11	2.68E+06	0.26
A	12 - 23	1.45E+06	0.24
Underburden	24 - 26	2.2E+06	0.25

Effect of Geomechanics - Gas Flooding EOR

Flow only

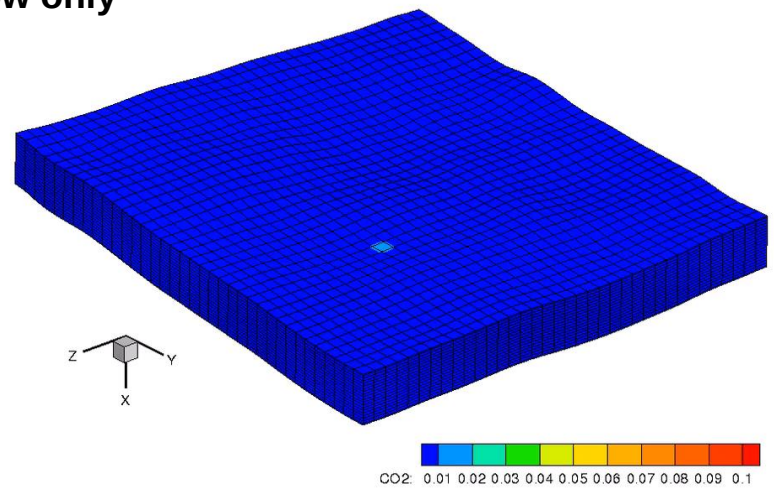

Coupled flow and geomechanics

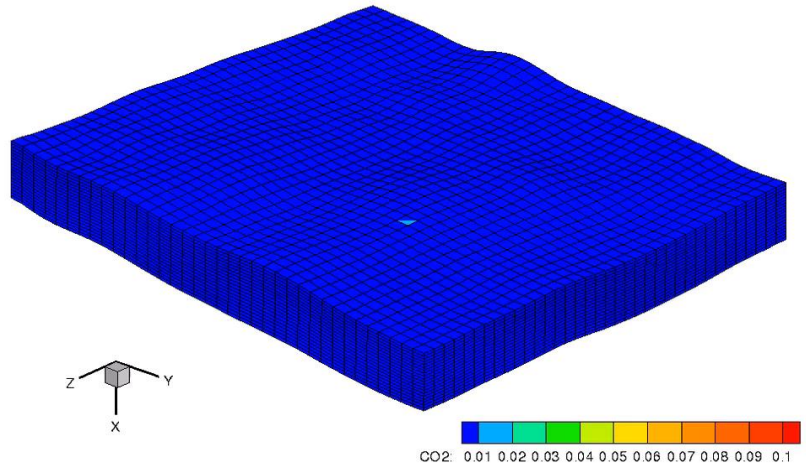

Cumulative gas storage

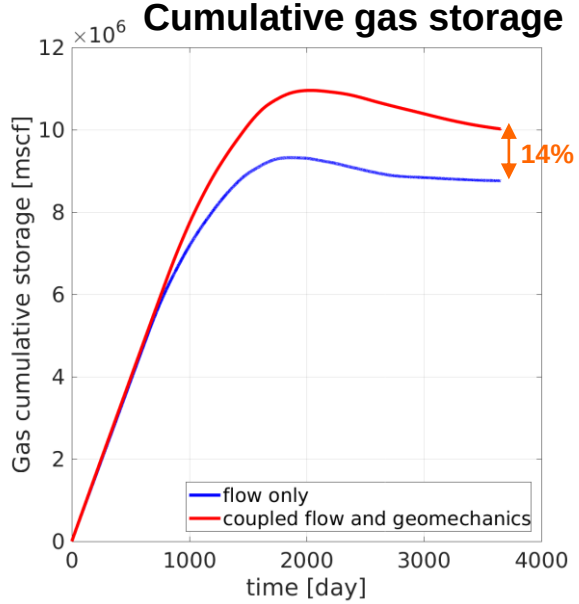

Cumulative oil production

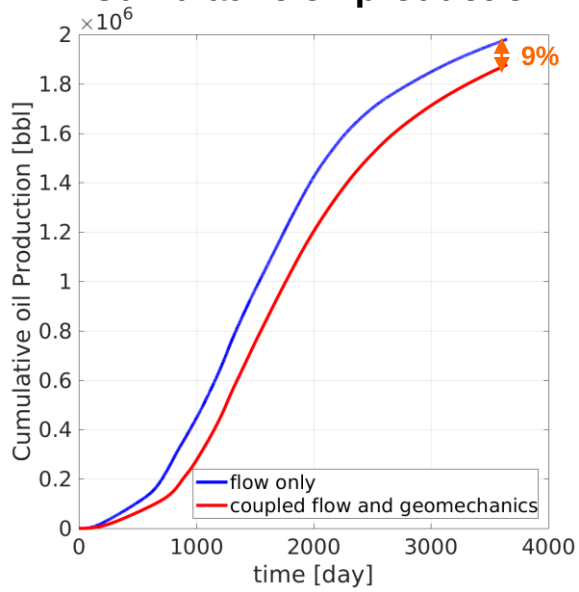

Injector 28F-01 BHP

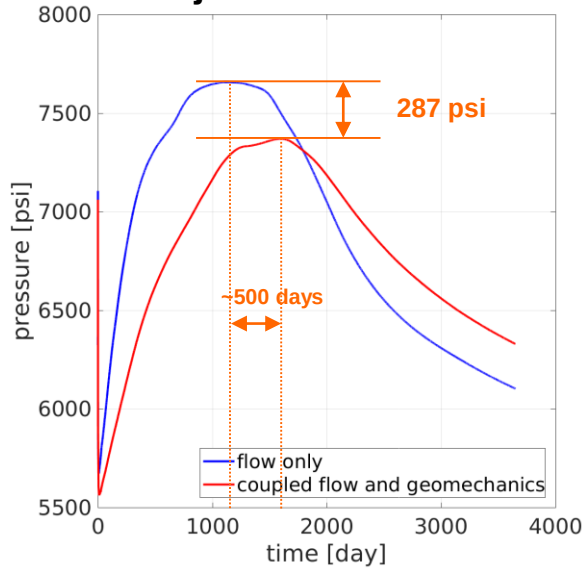

Caprock Integrity – Gas Flooding

Volumetric strain
~ 0- 0.016

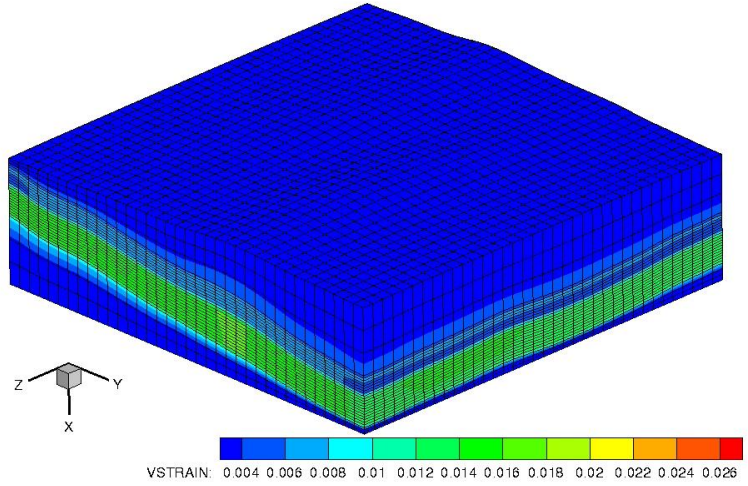

Vertical displacement
~ 0-0.34 ft

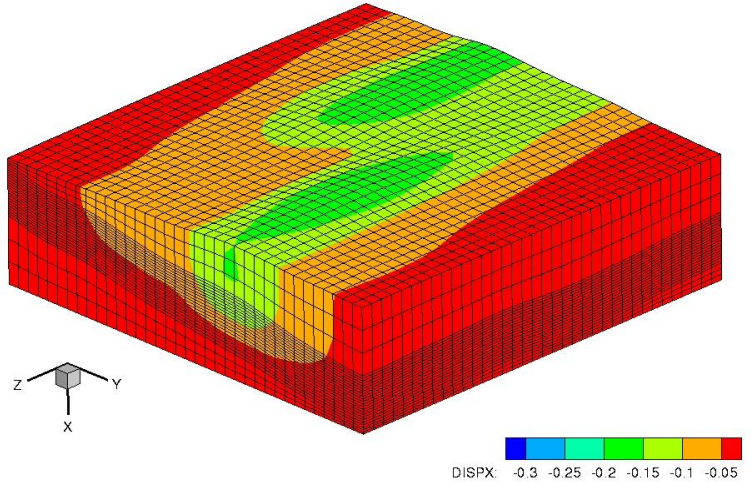

Pressure margin for inducing fracturing ~ 3000-5800 psi

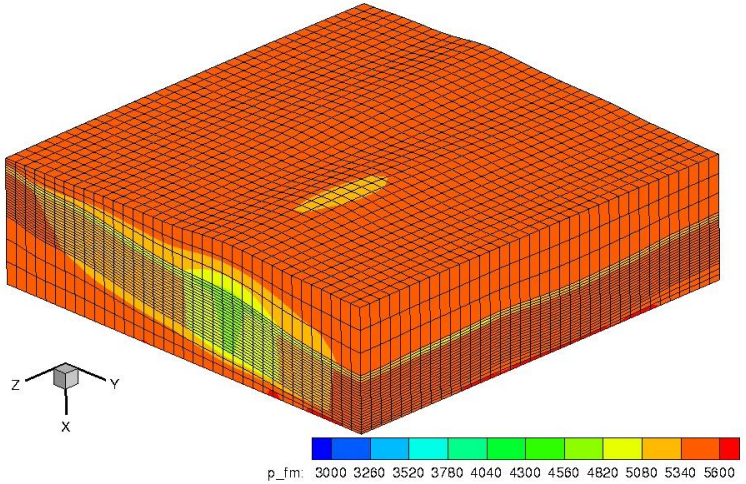

- **Pressure margin for inducing fracturing**

$$p_{fm} = p_{fc} - p \qquad p_{fc} = -\sigma_3^{tot}$$

Effect of Geomechanics - SAG EOR

Flow only

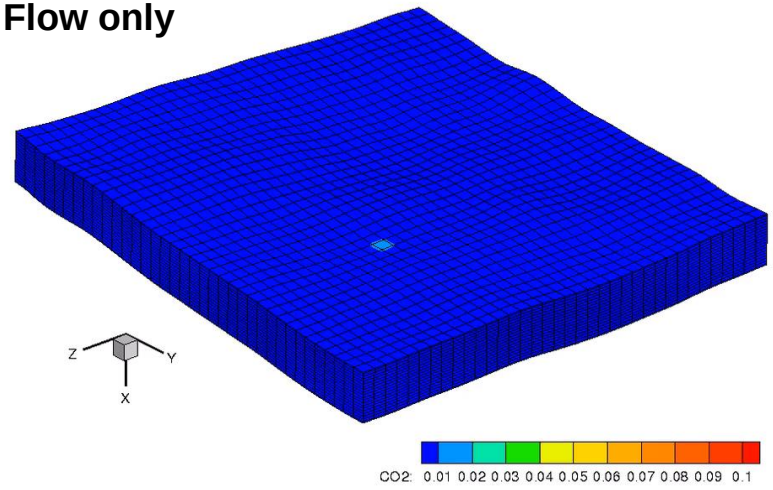

Coupled flow and geomechanics

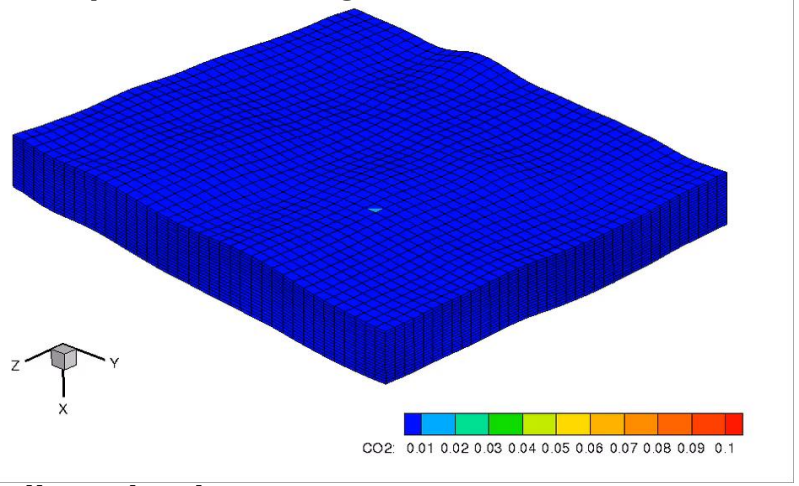

Cumulative gas production

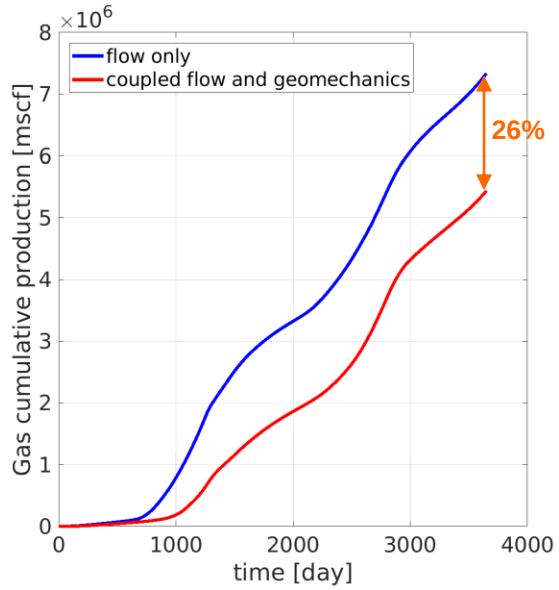

Cumulative oil production

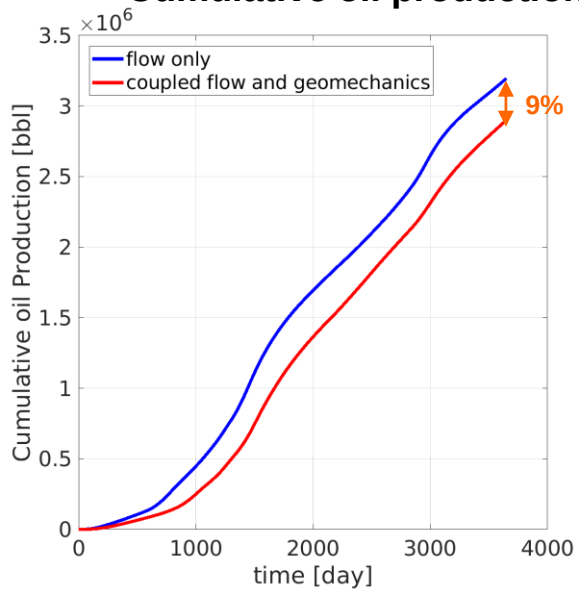

Injector 28F-01 BHP

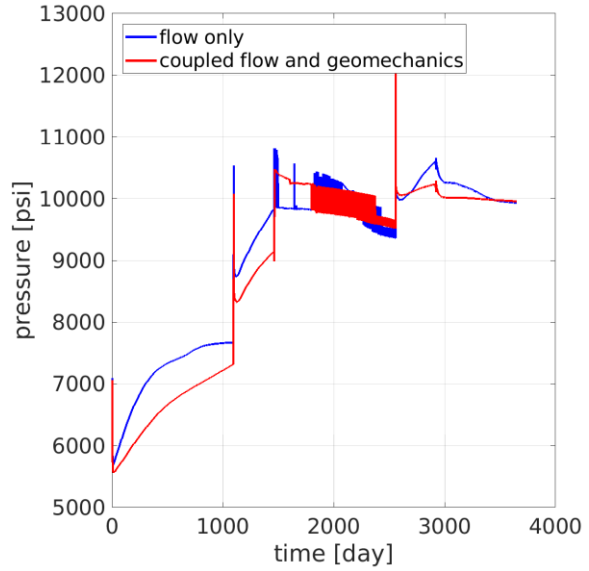

Caprock Integrity – SAG

Volumetric strain
~ 0 - 0.026

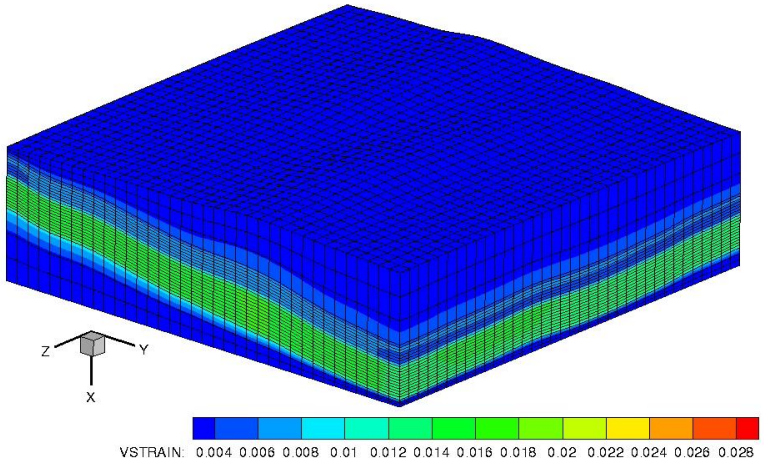

Vertical displacement
~ 0- 1.1 ft

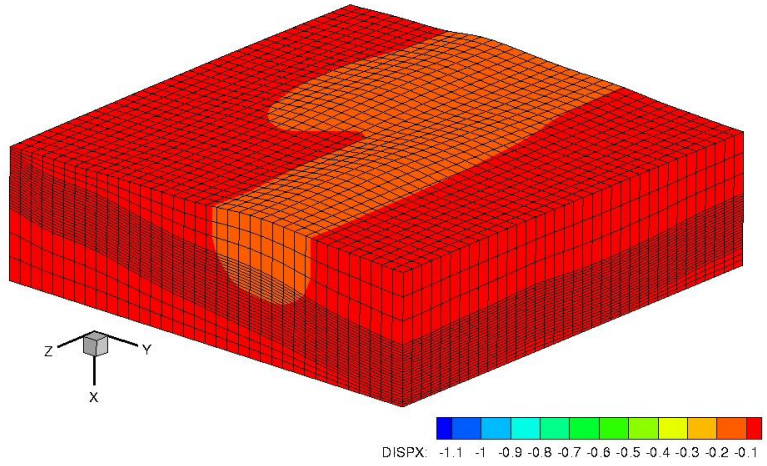

Pressure margin for inducing fracturing
~ 500 – 5500 psi

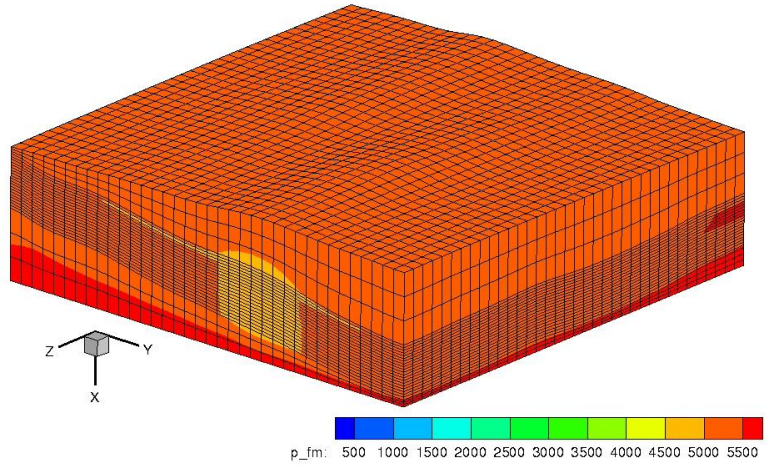

- ❑ Introduction
- ❑ Numerical Study of Gas Mobility Control Techniques in Cranfield
- ❑ Geomechanics Effects on Gas Mobility Control Techniques
- ❑ Optimization of Surfactant Alternating Gas (SAG) Process
- ❑ Conclusions

Forward Simulation Speedup: Three-Way Coupling

- Originally proposed for single phase flow by Dean et al. 2006
- Reformulated, analyzed and extended to compositional flow by Lu and Wheeler 2019

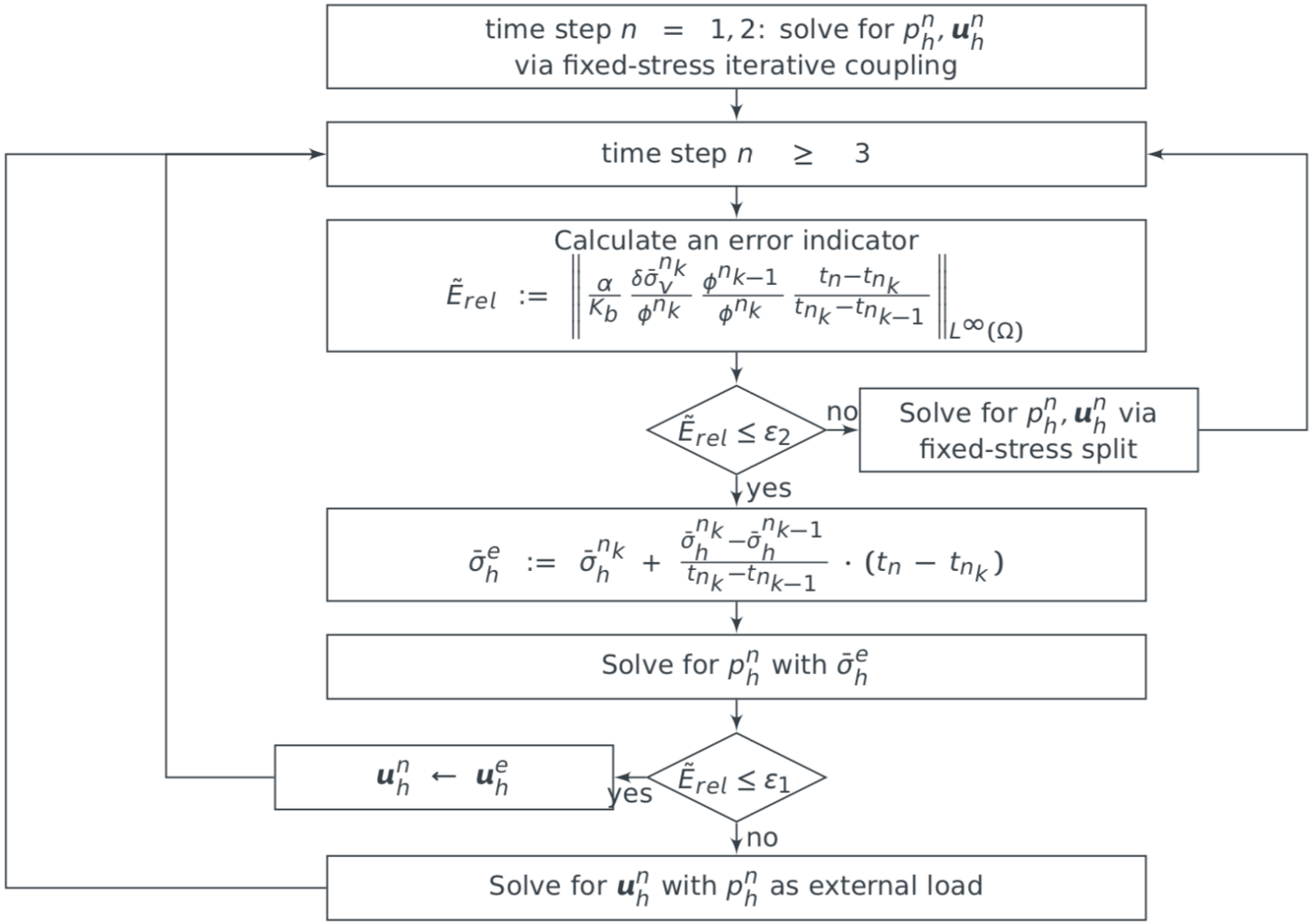

Three Way Coupling Applied to Field Scale SAG

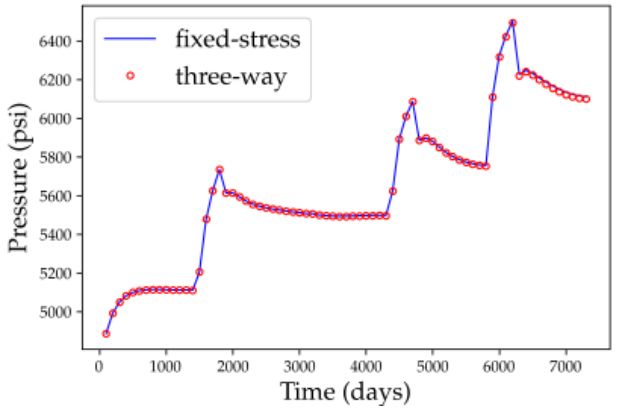

(a) pressure solution

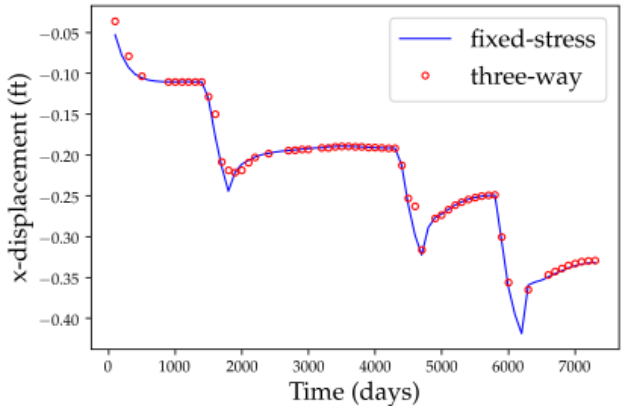

(b) *x*-displacement solution

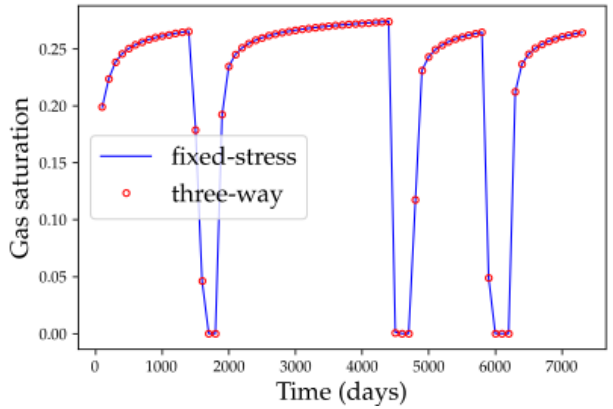

(c) gas saturation solution

Comparison of numerical results of SAG-assisted CO2 injection via different coupling schemes.

Technique	Time steps	Flow model time (s)	Mechanics model time (s)	CPU time (s)
Fixed-stress	142937	65496.906	262636.156	328133.062
Three-way	141152	64969.177	6633.925	71603.102

- Reduction of **78.2%** of CPU time comparing to fixed-stress
- Reduction of **97.5%** of mechanics model time

CMA-ES Optimization of Well Controls during SAG

SAG Injection Schedule:

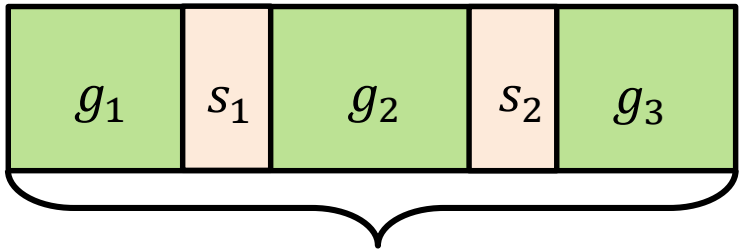

□ : surfactant ■ : CO_2

$$\max f(T_{g1}, T_{s1}, T_{g2}, T_{s2}, T_{g3}) := \text{FGIT} - \text{FGPT}$$
$$\text{s.t. } 0 \le T_{gi} \le 3, i = 1, 2$$
$$0 \le T_{si} \le 1, i = 1, 2$$
$$T_{g3} \ge 0$$
$$T_{g1} + T_{s1} + T_{g2} + T_{s2} + T_{g3} = 10$$

FGIT= Field cumulative CO_2 injection volume
FGPT= Field cumulative CO_2 production volume through boundary wells

Covariance Matrix Adaptation-Evolution Strategy

Algorithm 1 Evolution strategy stochastic search template to minimize $f : \mathbb{R}^n \to \mathbb{R}$

1: Initialize distribution parameters θ, set population size $\lambda \in \mathbb{N}$
2: **while** not terminate **do**
3: Sample distribution $P(x|\theta) \to x_1, \cdots, x_\lambda \in \mathbb{R}^n$
4: Evaluate $f(x_1), \cdots, f(x_\lambda)$
5: Update parameters $\theta \leftarrow F_\theta(x_1, \cdots, x_\lambda, f(x_1), \cdots, f(x_\lambda))$

- Multivariate normal distribution to sample new searching points follows the **maximum entropy principle**
- Rank-based selection leads to **maximum likelihood updates** for mean and covariance
- Update of the distribution parameters resembles the descent in direction of a sampled **natural gradient** of the expected objective function value
- Learning the **covariance matrix adaptation** is analogous to approximate the **inverse Hessian** in quasi-Newton methods
- Empirically, **linear (or exponential) convergence**
- Empirically **very successful for low dimensional problems**

Results: CMA-ES vs GA

- CMA-ES appears more efficient and robust than GA
- It achieves 27.6% higher CO_2 storage volume and 54.8% less water and surfactant consumption

Algorithm	Run #	Optimal solution	Opt. function value (MMSCF)
CMA-ES	1	(0.000, 0.903, 2.912, 0.000, 6.177)	2.558×10^4
CMA-ES	2	(0.000, 0.000, 0.006, 0.984, 9.010)	2.556×10^4
CMA-ES	3	(0.000, 0.936, 0.000, 0.000, 9.064)	2.557×10^4
GA	1	(0.080, 0.589, 1.950, 0.007, 7.374)	2.445×10^4
GA	2	(0.650, 0.847, 0.087, 0.231, 8.185)	2.511×10^4
GA	3	(0.573, 0.929, 0.597, 0.008, 7.893)	2.506×10^4

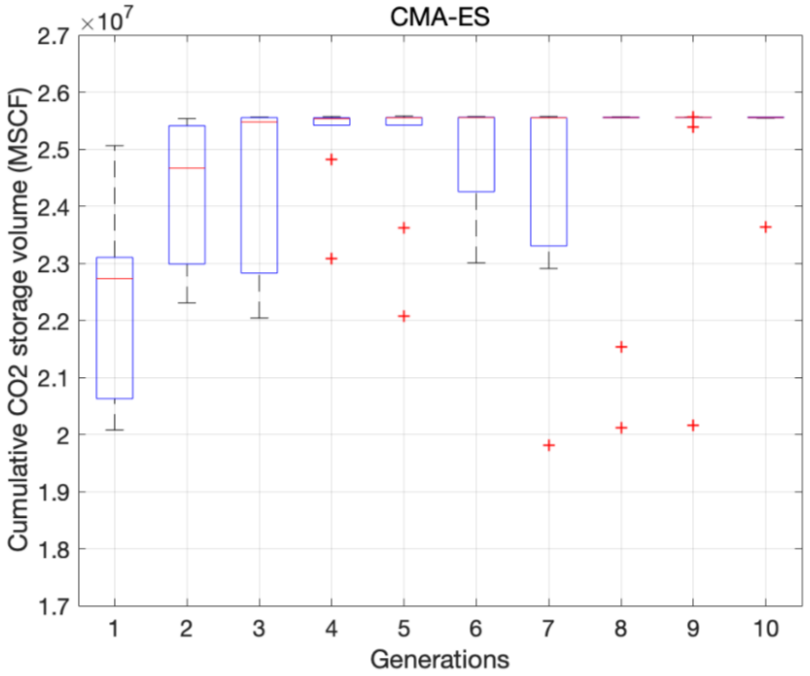

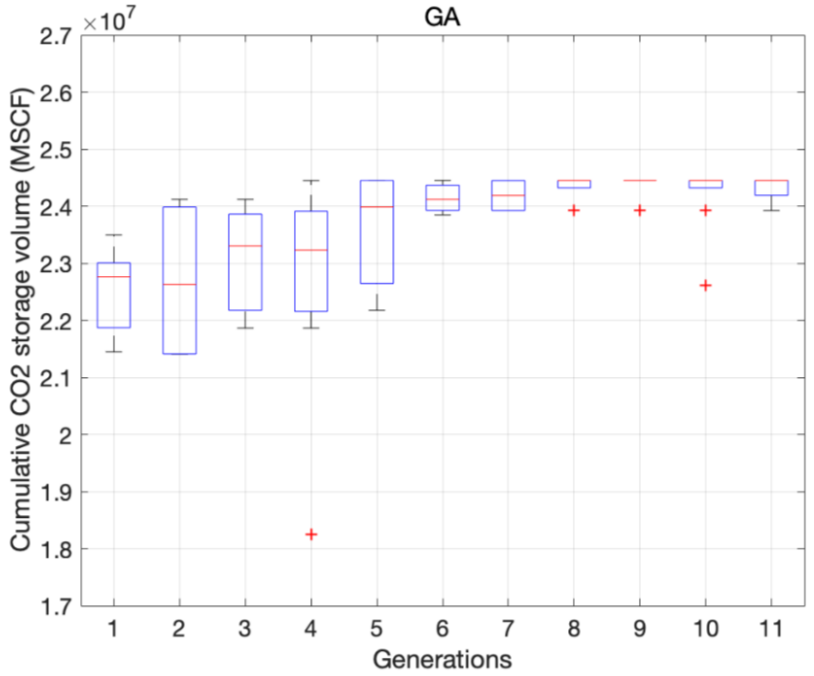

Conclusions

- Application of SAG can increase both CO2 storage volume and oil recovery significantly during carbon sequestration/EOR processes.
- Coupling geomechanics to the flow model predict less oil production but more CO2 storage due to pore volume expansion. The discrepancy in gas production is more significant in SAG operation (26.0%).
- The coupled compositional flow and geomechanics simulator provides a powerful tool for analyzing caprock integrity via quantification of the pressure margin for inducing fracturing.
- Three-way coupling scheme reduces computational time by 81% and 58% for continuous CO_2 injection and SAG-assisted CO_2 sequestration, respectively.
- CMA-ES optimization of well control for SAG achieves 27.6% higher CO_2 storage volume and 54.8% less water and surfactant consumption. The algorithm appears more efficient and robust than GA.

Thank You!

References:

Xueying Lu, Mary F. Wheeler, "*Three-Way Coupling of Multiphase Flow and Poromechanics in Porous Media*", under review with Journal of Computational Physics

Xueying Lu, Ben Ganis, and Mary F. Wheeler, " *Optimal Design of CO2 Sequestration with Three- Way Coupling of Flow-Geomechanics Simulations and Evolution Strategy*", SPE Reservoir Simulation Conference, 2019

Xueying Lu, Mohammad Lotfollahi, Ben Ganis, Baehyun Min and Mary F. Wheeler, "*An Integrated Flow-Geomechanical Analysis of Flue Gas Injection in Cranfield*", SPE Improved Oil Recovery Conference, 2018

M. Lotfollahi, I. Kim, M. R. Beygi, A. J. Worthen, C. Huh, K. P. Johnston, M. F. Wheeler, and D. A. DiCarlo. Foam generation hysteresis in porous media: Experiments and new insights. Transport in Porous Media, 116(2):687–703, 2017.

CSM CENTER FOR SUBSURFACE MODELING

ODEN INSTITUTE FOR COMPUTATIONAL ENGINEERING & SCIENCES

CSM CENTER FOR SUBSURFACE MODELING

Backup Slides

Compositional Cranfield Model

Numerical model of Cranfield field test	
Model type	Compositional model
Reservoir size	7200×7200×80 (ft)
Number of grid blocks	144×144×20
Initial water saturation	1.0
Initial reservoir pressure	4650 (psi)
Initial reservoir temperature	257 (°F)
Reservoir salinity	150,000 (ppm)

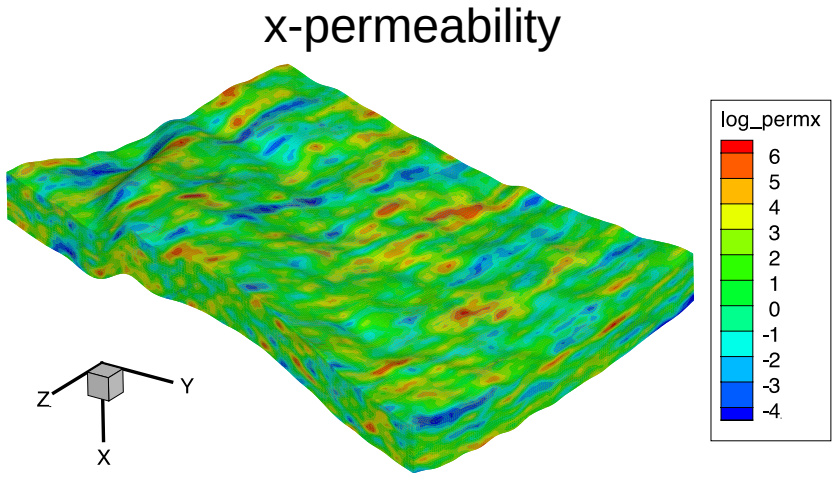

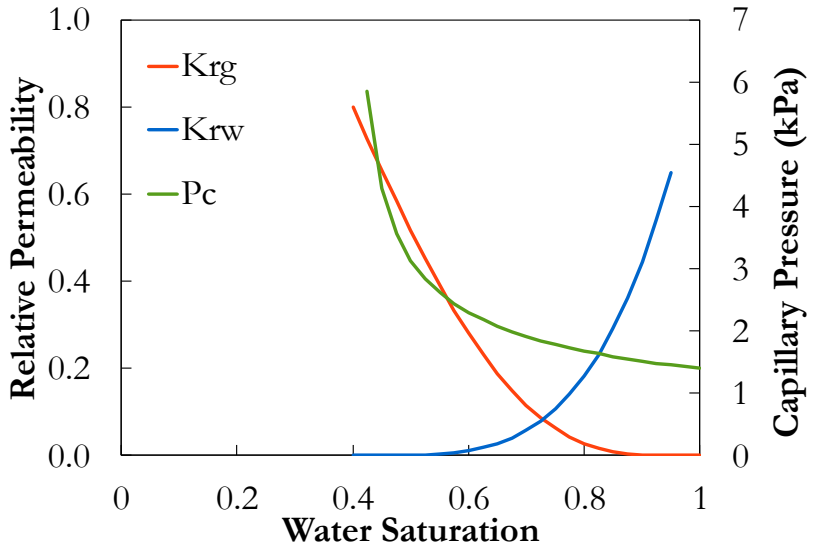

PVT data		
	CO_2	Brine
Critical temperature (°R)	547.56	1120.23
Critical pressure (psia)	1070.4	3540.9
Compressibility factor	0.255	0.2
Acentric factor	0.224	0.244
Molecular weight (g/g mol)	44.01	18.01
Volume-shift	-0.19	0.065
Binary interaction coefficients	0.09	0.09

(Delshad et al. 2013)

Genetic Algorithm

- Uses concepts from *evolutionary biology* (Goldberg, 1989)

Algorithm 1 Genetic Algorithm

1: **INITIALIZE** the parent population P_0 with N_{pop} solutions generated based on prior knowledge or by random. The initial offspring population $Q_0 = \varnothing$
2: **EVALUATE** each parent solution in P_0
3: **while** *termination condition is not achieved* **do**
4: $t \leftarrow t + 1$
5: **SELECT** N_{pop} superior solutions from the mating pool $R_t = P_{t-1} \bigcup Q_{t-1}$
6: **UPDATE** the parent population P_t with the selected solution,
7: **CROSSOVER** pairs of the parent solutions for creating N_{pop}-sized Q_t
8: **MUTATE** the resulting offspring population Q_t
9: **EVALUATE** each offspring solution in Q_t

Algorithm 2 Crossover

1: $i \leftarrow 1$
2: **while** $i < N_{pop}$ **do**
3: **GENERATE** a random probability $p_r \in [0, 1]$
4: **SELECT** two parent members $\mathbf{p}_i$ and $\mathbf{p}_{i+1}$
5: **if** $p_r < p_c$ **then**
6: **GENERATE** a crossover point $r_c \in \{1, 2, \cdots, N\}$
7: $\mathbf{q}_i \leftarrow (p_{i,1}, \cdots, p_{i,r_c}, p_{i+1,r_c+1}, \cdots, p_{i+1,N})^T$
8: $\mathbf{q}_{i+1} \leftarrow (p_{i+1,1}, \cdots, p_{i+1,r_c}, p_{i,r_c+1}, \cdots, p_{i,N})^T$
9: **else**
10: $\mathbf{q}_i \leftarrow \mathbf{p}_i$
11: $\mathbf{q}_{i+1} \leftarrow \mathbf{p}_{i+1}$
12: $i \leftarrow i + 2$

Algorithm 3 Mutation

1: $i \leftarrow 1$
2: **while** $i < N_{pop}$ **do**
3: **GENERATE** a random probability $p_r \in [0, 1]$
4: **if** $p_r < p_m$ **then**
5: **GENERATE** a mutation point $r_m \in \{1, 2, \cdots, N\}$
6: **GENERATE** the random mutation $q^*_{i,r_m} \in [q^{\min}_{r_m}, q^{\max}_{r_m}]$
7: $\mathbf{q}_i \leftarrow (q_{i,1}, \cdots, q_{i,r_m-1}, q^*_{i,r_m}, q_{i,r_m+1}, \cdots, q_{i+1,N})^T$
8: $i \leftarrow i + 1$

Optimization Setup

- Upscale

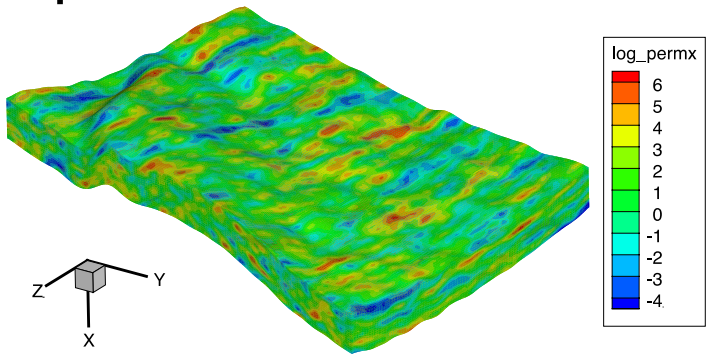

20x144x144 mesh

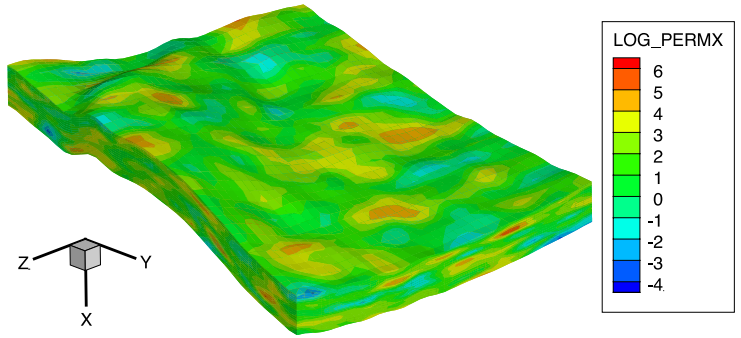

20x36x36 mesh

- Parallel scalability test

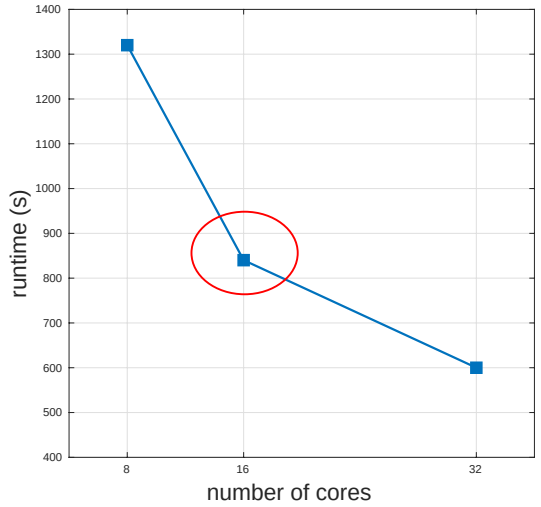

GA parameters	
Number of generations	10
Number of populations	20
Crossover probability	0.9
Mutation probability	0.1
Number of cores each experiment	16

EOR Example Reservoir Model

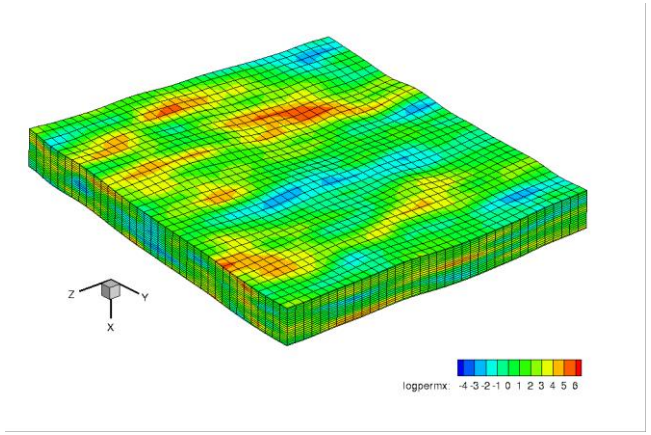

x-permeability

- Reservoir size: 80ft x 3600ft x 3600ft
- 3 layers of overburden and underburden
- 26x36x36 elements on hexahedral mesh
- Initial saturation: 40% oil, 60% water
- Initial pressure: 4650 psi

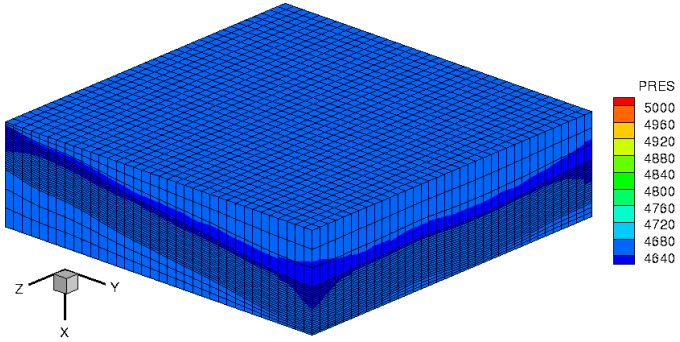

mesh

- Initial vertical stress 10054 psi, horizontal stress 7495 psi
- Normal traction of 10054 psi on the top face
- Zero normal displacements (roller boundary) on the rest five faces

Coupled Flow-Mechanics Data

Table 1: Equation-of-state parameters for different components used in the simulation study

	CO_2	C1	C3	C6	C7+	N2
Critical temperature (° R)	547.56	343.08	665.64	913.5	1380.0	226.56
Critical pressure (psi)	1070.38	667.19	615.76	477.03	162.0	492.32
Critical Z-factor	0.30234	0.287368	0.280294	0.268127	0.2916	0.2916
Acentric factor	0.225	0.008	0.152	0.275	0.85	0.04
Molecular weight (g/g mol)	44.01	16.04	44.09	86	282	28.013
Parachor	49	77	150.3	250.1	289.6	87
Initial mole fraction	0.0184	0.5376	0.1015	0.0728	0.2697	0.0

Table 2: Parameters for UTKR3P and UTHYST

k^0_{rwo}	0.5	$k^0_{rwg} = k^0_{rog}$	0.54	k^0_{row}	0.65	$k^0_{rgw} = k^0_{rgo}$	0.8
S_{org}	0.15	$S_{wrg} = S_{wro}$	0.4	S_{orw}	0.2	$S_{grw} = S_{gro}$	0.075
C_{1wo}	4.0	$C_{1wg} = C_{1og}$	4.0	C_{1ow}	2.38	$C_{1gw} = C_{1go}$	2.2
C_{2*}	0	$S_{wc} = S_{oc} = S_{gc}$	0	L_g	4	m_g	2.25

Coupled Flow-Mechanics Data

Table 3: Parameters for the foam model

Maximum resistance factor, FMMOB	100
Reference water saturation in dry-out calculation, FMDRY	0.43
Factor governing abruptness of dry-out calculation, EPDRY	100
Reference rheology capillary number, FMCAP	1E-07
Shear-thinning exponent, EPCAP	0
Watergas interfacial tension, (dyne/cm), IFTGW	5

Table 4: Young's modulus and Poisson's ratio for the Cranfield model, courtesy to White et al., 2017

Facies	Layers	E (psi)	ν
Overburden	1 - 3	2.2E+06	0.25
C	4 - 6	1.45E+06	0.31
B	7 - 11	2.68E+06	0.26
A	12 - 23	1.45E+06	0.24
Underburden	24 - 26	2.2E+06	0.25